



Deposited via The University of Sheffield.

White Rose Research Online URL for this paper:

<https://eprints.whiterose.ac.uk/id/eprint/200528/>

Version: Accepted Version

Article:

Gaspar, T.A.V., Jacobsz, S., Smit, G. et al. (2024) Centrifuge modelling of piled foundations in swelling clays. *Canadian Geotechnical Journal*, 61 (1). pp. 46-58. ISSN: 0008-3674

<https://doi.org/10.1139/cgj-2022-0449>

© 2023 The Authors. Except as otherwise noted, this author-accepted version of a journal article published in *Canadian Geotechnical Journal* is made available via the University of Sheffield Research Publications and Copyright Policy under the terms of the Creative Commons Attribution 4.0 International License (CC-BY 4.0), which permits unrestricted use, distribution and reproduction in any medium, provided the original work is properly cited. To view a copy of this licence, visit <http://creativecommons.org/licenses/by/4.0/>

Reuse

This article is distributed under the terms of the Creative Commons Attribution (CC BY) licence. This licence allows you to distribute, remix, tweak, and build upon the work, even commercially, as long as you credit the authors for the original work. More information and the full terms of the licence here: <https://creativecommons.org/licenses/>

Takedown

If you consider content in White Rose Research Online to be in breach of UK law, please notify us by emailing eprints@whiterose.ac.uk including the URL of the record and the reason for the withdrawal request.

1 **Centrifuge modelling of piled foundations in swelling clays**

2

3 Author 1

- 4 • T.A.V. Gaspar, PhD (Pretoria) – corresponding author
5 • Department of Civil Engineering, University of Pretoria, Pretoria, South Africa
6 • <https://orcid.org/0000-0002-3746-2714>
7 • Present address:
8 ○ Department of Civil and Structural Engineering, University of Sheffield, United
9 Kingdom
10 ○ Sheffield, S1 3JD

11 Author 2

- 12 • S.W. Jacobsz, PhD (Cantab)
13 • Department of Civil Engineering, University of Pretoria, Pretoria, South Africa
14 • <https://orcid.org/0000-0002-7439-2276>

15 Author 3

- 16 • G. Smit, PhD (Southampton)
17 • Department of Civil Engineering, University of Pretoria, Pretoria, South Africa

18 Author 4

- 19 • A.S. Osman, PhD (Cantab)
20 • Department of Engineering, Durham University, United Kingdom
21 • <https://orcid.org/0000-0002-5119-8841>

22

23 Full contact details of corresponding author

- 24 • Email address 1: t.a.gaspar@sheffield.ac.uk
25 • Email address 2: tav.gaspar@gmail.com
26 • Mobile: +447488560650

27

28

29

30

31

32

33

34 **Abstract**

35 A study aimed towards assessing the variation in shaft capacity of piled foundations in swelling
36 clays is presented. At the clay's in-situ water content, the results of pull-out tests on short
37 length piles revealed no dependency of shaft capacity on overburden stress. Conversely, after
38 achieving a targeted value of swell, a strong dependency on overburden stress was observed.
39 In upper portions of the profile where swell can occur relatively freely, swell-induced softening
40 results in a reduction in pile shaft capacity. However, at greater depths where swell is largely
41 suppressed, so too are the effects of swell-induced softening. For this reason, shaft capacity
42 at depth was found to remain relatively constant before and after swell. The results of an
43 instrumented pile test revealed an overriding dependency of lateral induced swell pressure on
44 the magnitude of heave which has occurred. Irrespective of the level of overburden stress,
45 lateral pressures against the pile were found to increase at early stages of the swelling
46 process, but then reduce as swell continued and softening began to occur. Such a result
47 highlights the importance of specifying the level of swell at which shaft capacity should be
48 assessed if a conservative design is to be obtained.

49

50 **Keywords: expansive soils; centrifuge modelling; piles and piling; partial saturation**

51

52 **List of notations**

53 e void ratio

54 N centrifuge model scaling factor

55 \bar{p} net-mean stress

56 s suction

57 S_r degree of saturation

58

59

60 **Introduction**

61 The severe economic implications associated with construction on expansive clays (Jones
62 and Holtz 1973; Jones and Jefferson 2012) have necessitated the implementation of
63 specialised foundation solutions. Measures taken to mitigate the effects of this problem soil
64 can broadly be divided into three categories, namely soil treatment or replacement,
65 construction directly on the expansive profile and, isolation of the superstructure from the
66 expansive profile.

67

68 Removal and replacement is generally a feasible approach if the depth of expansive material
69 is shallow (approximately 2 m deep) and when suitable inert material is readily available
70 (Byrne *et al.* 2019). Alternatively, the soil can be 'treated' by pre-wetting the profile such that
71 swell occurs before construction, thus limiting structural distress. Drawbacks of this approach
72 include the time taken for the soil to reach an equilibrium moisture content, and the uncertainty
73 of future changes in moisture throughout the lifetime of the structure (Byrne *et al.* 2019).
74 Arguably the most common approach for foundation design on swelling clays is to utilise a
75 stiffened raft foundation (Byrne *et al.* 2019; Charlie *et al.* 1985; Li *et al.* 2014; Pellissier, 1997).
76 The rationale behind such a foundation type is to prevent differential movements across the
77 foundation, thereby limiting structural distress. Isolation of the superstructure from the
78 underlying expansive soil is the most expensive of the three approaches mentioned. The
79 approach typically involves the use of piled foundations extending either to bedrock where
80 they can be socketed, or to a stable soil horizon where the foundation can be anchored using,
81 for example, enlarged base piles (Byrne *et al.* 2019). These piles are then used to support a
82 suspended foundation which is completely isolated from the underlying soil. The gap provided
83 between the suspended foundation and the ground level provides space for the soil to swell
84 into, without affecting the superstructure.

85 Piles used in this construction method can be subjected to large uplift forces due to heaving
86 soil around the pile. To ensure cracking of the piles does not occur, they can either be
87 adequately reinforced, 'sleeved' (provided with a slip layer) or a combination of these

88 measures can be implemented (Fleming *et al.* 2009). However, in cases where the expansive
89 profile is particularly deep, 'sleeving' and/or socketing into bedrock can become
90 uneconomical. In Kimberley, South Africa, expansive profiles have been found to extend to a
91 depth of up to 30 m (Byrne *et al.* 2019). Other instances of deep expansive profiles have also
92 been reported in Sudan, where it is not uncommon to have expansive profiles extending to
93 greater than 10 m (Elsharie 2012).

94

95 While this foundation type can double the cost of construction (Jennings and Kerrich 1962), if
96 applied correctly, it can result in almost no foundation movements. This foundation type is
97 however, not necessarily a fail-safe approach. Under-prediction of heave can result in the gap
98 between the clay and suspended foundation swelling closed, thereby resulting in uplift of the
99 superstructure.

100

101 A case study where such a design proved to be inadequate was reported by Meintjes (1991).
102 The study reported structural damage due to excessive heave, despite the foundation being
103 designed to have a void of 150 mm between the grade beam and pile cap, and under-
104 reamed/enlarged base piles extending to a depth of 7.7 m.

105

106 Blight (1984) presented the findings of another case study where suspended foundations were
107 used for several buildings at a thermal power plant. While the initial heave calculated for this
108 site was in the order of 120 mm (Blight 1984), this was a gross underestimation of what was
109 observed. Prior to construction, removal of vegetation resulted in rising of the water table,
110 causing far greater heave than what was initially estimated, thereby closing the gap between
111 ground level and the suspended foundation. Some remedial measures implemented at this
112 site have involved increasing the gap between the suspended slabs and the expansive clay
113 to 300 mm. It has been noted that at some buildings at the power plant, these voids have
114 swelled closed yet again (Day 2017).

115

116 This particular case study led to a number of useful investigations on this method of
117 construction. Blight (1984) conducted full-scale pull-out tests on short length piles before and
118 after wetting the profile for a period of 3–4 weeks. His results indicated that an increase in pile
119 pull-out (shaft) capacity was observed after wetting. This finding was in direct contradiction
120 with a study conducted by Elsharief *et al.* (2007) for pile load tests conducted in Sudan. An
121 explanation for this contradiction is that, while the swelling process can produce an increase
122 in lateral stresses against a pile shaft, swell induced softening of the clay (Gens and Alonso,
123 1992) results in a reduction of shear strength which can ultimately reduce shaft capacity. This
124 softening can be viewed as resulting due to a reduction in matric suction, or the structural
125 realignment occurring due to macroscopic volumetric change (i.e. swell) (Gens and Alonso
126 1992). If an engineer is to produce a conservative design for such foundation types, an
127 understanding of these counteracting mechanisms is crucial.

128

129 In an effort to investigate the effects of these mechanisms, Smit *et al.* (2019) presented the
130 results of centrifuge pile pull-out tests. The study involved pull-out tests of bored piles installed
131 in an expansive profile at:

132

- 133 a) the clay's in-situ water content and
- 134 b) after allowing swell to occur.

135

136 The results of this study indicated that, after achieving a targeted magnitude of swell, the pull-
137 out capacity of piles reduced by between 57 and 67% when compared to their capacities at
138 the clay's in-situ water content.

139

140 While the results of this preliminary study indicate average shaft friction along the full length
141 of the pile, they give no information on the variation in shaft (pull-out) capacity with depth.
142 Furthermore, such tests investigate the consequence of the two counteracting mechanisms
143 (softening and changes in lateral stresses) without measuring these quantities directly. This

144 study presents a series of centrifuge models aimed to address these shortcomings and
145 provide insights into the aforementioned counteracting mechanisms.

146

147 The first three tests presented in this study involve pull-out tests conducted on short length
148 piles (plugs) at various depths throughout the clay profile. The intention of these tests is to
149 investigate the effect of confinement on the evolution of pile shaft capacity before and after
150 swell. The final test incorporates the use of an aluminium pile, instrumented to measure the
151 change of lateral pressures on the pile shaft throughout the swelling process. This
152 instrumented pile test also included in-flight penetration tests at the clay's in-situ moisture
153 content and after allowing swell to occur. The purpose of this strength characterisation was to
154 obtain an indication of the magnitude of swell-induced softening.

155

156 ***Basic soil classification***

157 The material tested in this study was a highly expansive clay, sampled from the Limpopo
158 province of South Africa, 350 km northeast of Pretoria. The material was sampled from the
159 upper 1.5 m of the profile and can be described as a stiff, fissured and slickensided black clay
160 containing fine nodular calcrete (Day 2020).

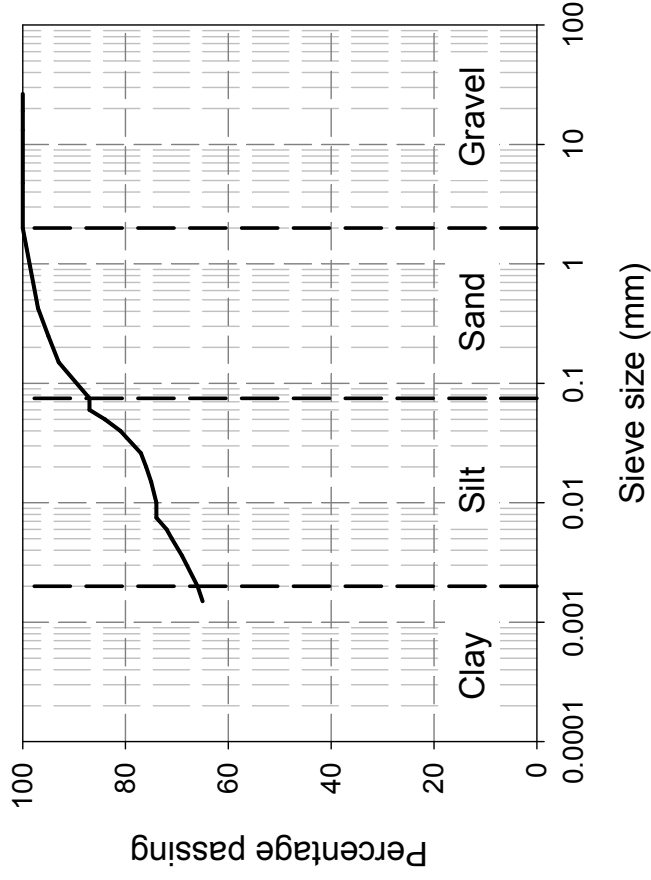
161

162 Basic classification tests were performed to establish the soil's particle size distribution (by
163 method of sieving (ASTM 2017a) and hydrometer (ASTM 2017b)), Atterberg limits (ASTM
164 2017c) and specific gravity (ASTM 2014a). These results, as well as the unified soil
165 classification (ASTM 2017d) are presented in Fig. 1 and Table 1. X-ray diffraction testing to
166 determine the mineralogical composition of the clay was performed on the same site by a
167 previous researcher, the results of which are shown in

168 Table 2

169

OPEN ACCESS: This work (the Author’s Accepted Manuscript) is licensed under a Creative Commons Attribution 4.0 International License (CC BY 4.0), which permits unrestricted use, distribution, and reproduction in any medium, provided the original author(s) and source are credited.



170

171

172

173

Fig. 1. Particle size distribution

Table 1. Soil classification data

Liquid limit (%)	92
Plasticity index	55
Linear shrinkage (%)	25.5
Activity	0.8
Specific gravity	2.65
Unified soil classification	CH

174

175

176

177

178

179

180

181

182 **Table 2. Mineralogical composition based on X-ray diffraction (after Moses 2008)**

Mineral	Composition (%)
Smectite	58
Palygorskite	19
Calcite	5
Plagioclase	5
Quartz	4
Enstatite	4
Kaolinite	3
Diopside	2

183

184 ***Characterisation of swell properties***

185 The mechanical properties of both compacted and undisturbed samples of the clay considered
 186 in this study was presented by Gaspar *et al.* (2022). The following section presents a summary
 187 of the oedometer tests conducted to quantify the swell properties of the tested clay. For the
 188 swell tests, data is presented for both compacted and undisturbed specimens (prepared from
 189 block samples). In doing so, the extent to which the laboratory prepared specimens replicated
 190 the undisturbed swell behaviour could be assessed.

191

192 Recognising the difficulties associated with preserving the fissured macrofabric of expansive
 193 clays during the sampling process, the preparation procedure implemented was aimed
 194 towards introducing a certain degree of ‘fissuring’ for samples prepared in the laboratory. This
 195 was accomplished by breaking down intact lumps of clay with a cheese grater at their in-situ
 196 water content (approximately 31%) and statically compacting the broken-down clay to a
 197 targeted dry density of 1350 kg/m³. These initial conditions were selected as they are
 198 representative of the measured in-situ properties of the clay after the dry season. The rationale
 199 for targeting properties related to this season is that they present the most critical case if swell

200 properties are to be measured (i.e. assessing the soil in its driest practical state allows for the
201 largest estimates of swell magnitude and swell pressure to be obtained).

202

203 This preparation procedure differs slightly from more conventional approaches whereby air-
204 dried soil is mixed with a predetermined quantity of water, allowed to equilibrate, and
205 compacted to a target dry density (Monroy *et al.* 2015; Manca *et al.* 2016). The drawback of
206 this more conventional approach, however, is that it results in a fabric with macropores which
207 are relatively isolated. This is in contrast to the fabric type more commonly associated with
208 expansive clays which consists of a series of interconnected pores (i.e. fissures) that more
209 easily facilitate the ingress of water.

210

211 To investigate the swell properties of the compacted and undisturbed specimens, a series of
212 *wetting after loading tests* (ASTM 2014b), sometimes referred to as *swell under load* tests,
213 were conducted at various applied stresses. Such tests involve placing an unsaturated sample
214 into the oedometer, applying a predetermined stress (referred to as the soaking stress) and
215 then flooding the housing with distilled water. As the sample is inundated, volumetric changes
216 are monitored until such point that these changes become negligible. Once volumetric
217 changes cease, the sample is considered as having reached a state of zero suction (Schreiner
218 1988) and the final volumetric strain is noted for that stress level. Table 3 presents the initial
219 sample properties for the oedometer swell tests. Fig. 2 illustrates the results of wetting after
220 loading tests for both the compacted and undisturbed specimens conducted at several values
221 of applied vertical stress. Linear regression curves have also been superimposed onto the
222 dataset for both the compacted and undisturbed samples.

223

224

225

226

227

228 **Table 3. Initial sample properties for oedometer swell tests**

Description	Soaking stress (kPa)	Void ratio, e	Gravimetric water content, w (%)	Degree of saturation, S_r (%)	Dry density (kg/m^3)
Compacted	12.5	0.969	33.6	91.9	1346
Compacted	25	0.971	33.6	91.6	1344
Compacted	50	0.908	30.3	88.5	1389
Compacted	100	0.938	32.2	90.9	1367
Compacted	200	0.973	34.6	94.4	1343
Compacted	300	1.037	34.6	88.6	1301
Compacted	400	1.027	34.6	89.4	1307
Undisturbed	12.5	0.939	31.5	89.0	1367
Undisturbed	25	0.888	30.3	90.5	1403
Undisturbed	50	0.817	29.5	95.6	1459
Undisturbed	100	0.889	30.2	90.2	1403
Undisturbed	200	0.901	29.9	87.8	1394
Undisturbed	300	0.992	30.3	81.0	1331
Undisturbed	400	1.020	32.0	83.2	1312
Undisturbed	500	1.068	30.8	76.3	1281

229

230

OPEN ACCESS: This work (the Author's Accepted Manuscript) is licensed under a Creative Commons Attribution 4.0 International License (CC BY 4.0), which permits unrestricted use, distribution, and reproduction in any medium, provided the original author(s) and source are credited.

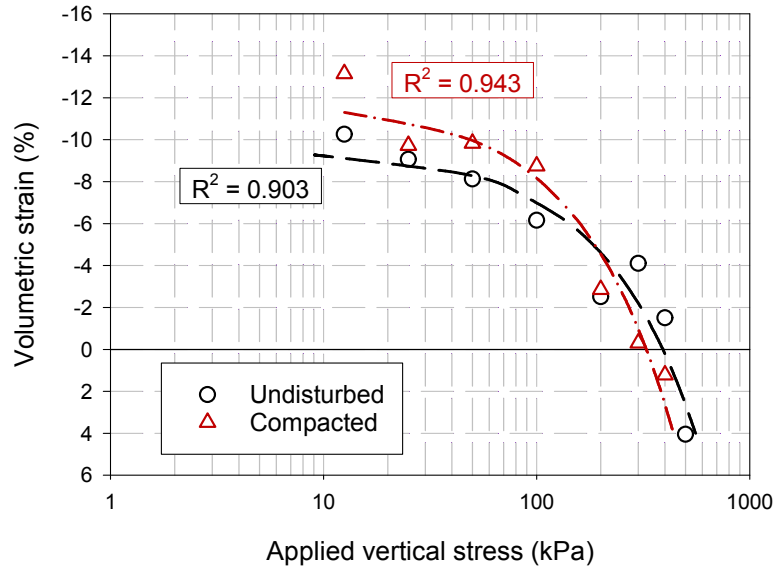


Fig. 2. Soaking under load curves for compacted and undisturbed samples

231

232

233

234 From Fig. 2 it can be seen that the measured swell properties of the compacted and
 235 undisturbed specimens are similar. Not only was the magnitude of swell achieved at all
 236 soaking stresses similar for the compacted and undisturbed samples, but the swell pressure
 237 also remained close. Using the regression curves plotted in Fig. 2, the stress required to
 238 achieve 0% volumetric change was 329 and 392 kPa for the compacted and undisturbed
 239 specimens respectively. Such results illustrate that the sample preparation procedure
 240 implemented was able to retain key swell characteristics of the undisturbed material. In light
 241 of this finding, the same approach was implemented in the preparation of the centrifuge
 242 models presented in the following section. It should also be highlighted that Gaspar et al.
 243 (2023) also reported the saturated hydraulic conductivity (k_{sat}) to be in the range of 10^{-9} - 10^{-12}
 244 m/s. These values were obtained by applying consolidation theory ($k_{sat} = c_v \cdot m_v \cdot \gamma_w$) to calculate
 245 k_{sat} from a consolidation test on a sample reconstituted at 1.1 times the soil's liquid limit.

246

247 **Model descriptions**

248 This section provides details of the centrifuge tests conducted in this study. First, a description
 249 of the clay profile and its preparation is provided. Additionally, aspects of the model layout

250 which are common to all tests are outlined. Thereafter, specific reference is made to the
251 position of piles within the clay profile, as well as the sequence that was followed for each
252 individual test. Unless otherwise stated, all dimensions provided in figures are in model scale.
253 Full-scale (prototype) lengths can be obtained by multiplying model dimensions by the model
254 scaling factor ($N=30$).

255

256 The centrifuge tests described in this study modelled an expansive soil profile comprising of a
257 stack of 5 clay layers (50 mm thick), statically compacted to a targeted dry density and
258 gravimetric water content of 1350 kg/m^3 and 31% respectively (the average in-situ values
259 determined from site investigations). It should be noted that at this state, the clay layers had
260 a matric suction of approximately 2 MPa. The clay layers were separated by needle punched,
261 non-woven geotextiles. The inclusion of geotextiles in the centrifuge models presented is to
262 facilitate the rapid ingress of water. Additionally, the geotextiles were sized such that hydraulic
263 contact could be maintained between geotextiles separating the clay layers, and the adjacent
264 water wells (described at the end of this paragraph). By controlling the length of the respective
265 geotextiles, an effort was made to avoid any anchorage of the geotextiles at their ends such
266 that they were able to move freely in the vertical direction as swell occurred, and not provide
267 stiffness to the profile. The five clay layers were laterally restrained in position by two
268 perforated steel plates, covered with the same geotextile used to separate the clay layers. The
269 two spaces on either side of the model were used as water wells to facilitate the ingress of
270 water. All tests presented in this study were performed at a centrifugal acceleration of 30 g.

271

272 The layout of the first two tests presented in this study, shown in Fig. 3, were identical and
273 incorporated 4 short-length piles (plugs) installed at various depths. For Test 1, the plugs were
274 pulled out of the profile at the clay's in-situ water content. In this study the "pull-out" capacity
275 is defined as the force required to mobilise peak shaft resistance between the bored piles and
276 surrounding clay. Water was subsequently introduced into the strongbox through inlets at the
277 bottom of the model until the water level was approximately 20 mm above the surface of the

278 top layer. Once the flooding process was complete, every clay layer had access to water on
279 all four boundaries (top, bottom and sides). The front and back of the model were confined
280 between the strongbox's glass window and an aluminium partition plate. After achieving the
281 targeted value of swell, ≈ 6.8 mm model scale, (as predicted by the Van der Merwe (1964)
282 empirical prediction method for a clay of *very high potential expansiveness*), the plugs were
283 pulled for a second time.

284

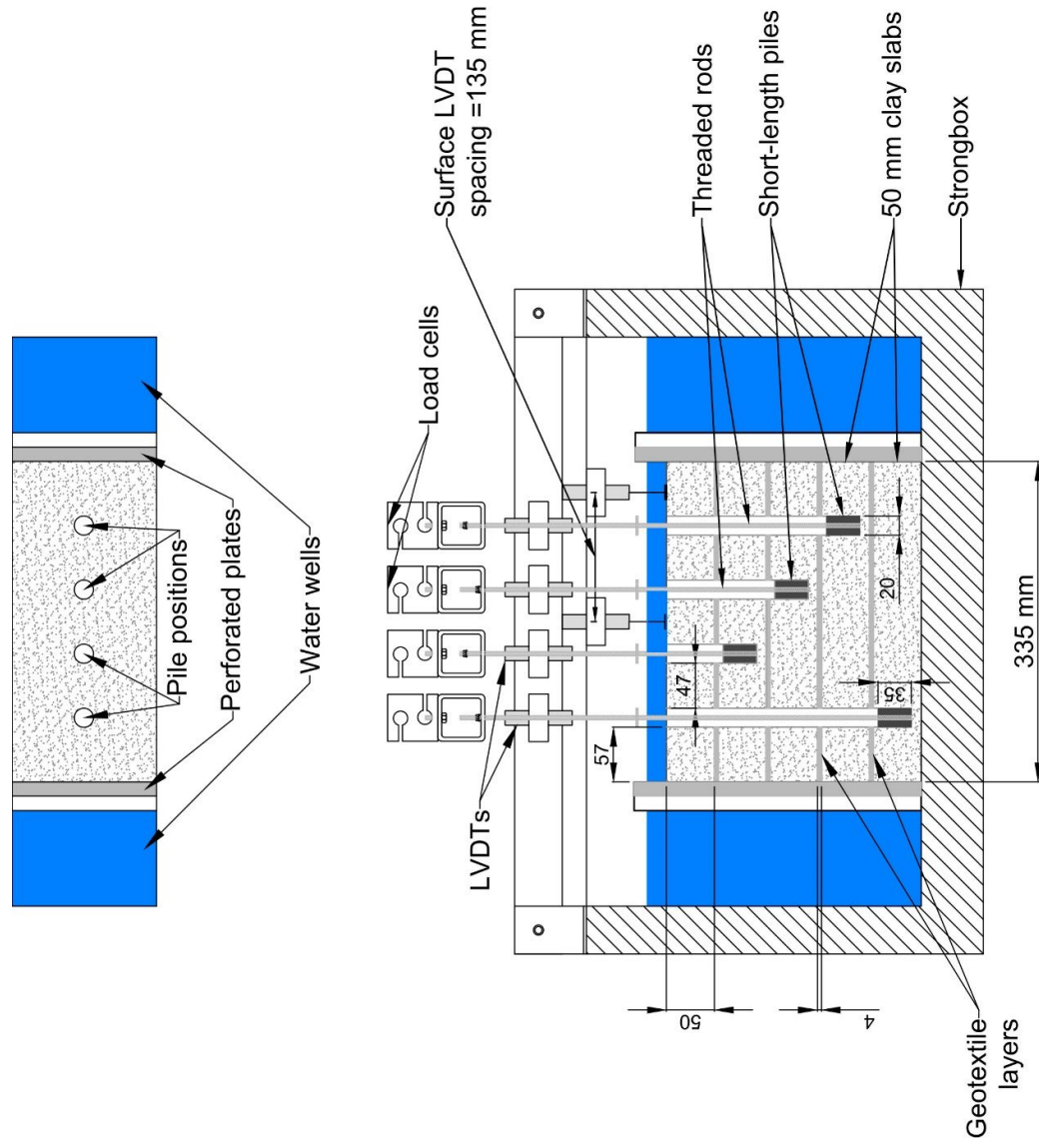
285 For the second test presented, pull-out tests were only conducted after the targeted swell was
286 achieved. From Fig. 3 it can be seen that the augered holes above the short length piles were
287 unsupported. As a result, clay was able to swell behind the plug as the strongbox was flooded.
288 To investigate the effect of the augered holes swelling closed above the plugs, a final pull-out
289 test was conducted whereby an aluminium tube was used to support the holes during swell
290 (all other aspects of the model layout remaining unchanged). The plugs were then pulled out
291 at the same magnitude of vertical swell as was done for the previous tests. An illustration of
292 the augered hole support is presented in Fig. 4. As shown in Fig. 4, a gap of 5 mm was left
293 between the top of the piles and the aluminium tube. The purpose of this gap was to ensure a
294 that the peak shaft resistance of the piles could be mobilised before making contact with the
295 supporting tube. Furthermore, the tube was clamped at the surface to ensure that this gap
296 was maintained, even as the soil swelled.

297

298 For all three pull-out tests, plugs were cast from a rapid hardening grout with a 4 mm stainless
299 steel threaded rod at their centres. Comparisons of material properties of this grout with a
300 scaled concrete mix developed for centrifuge modelling (Louw *et al.* 2020) indicated that the
301 two materials had similar mechanical properties (Gaspar 2020). Furthermore, the load and
302 displacement of piles throughout testing were monitored using load cells and linear variable
303 differential transformers (LVDTs) respectively in all three tests. It should be noted that for all
304 three pull-out tests, each short-length pile in a given model was pulled out individually (rather
305 than all piles in a model being pulled at the same time). It was therefore possible to ensure

306 that the testing of a single pile did not induce displacements throughout the model which might
 307 affect testing of adjacent piles. Additionally, LVDTs were also used to measure swell
 308 magnitude at the surface of the clay profile.

309



310

311

312

Fig. 3. Model layout for Tests 1 and 2

OPEN ACCESS: This work (the Author's Accepted Manuscript) is licensed under a Creative Commons Attribution 4.0 International License (CC BY 4.0), which permits unrestricted use, distribution, and reproduction in any medium, provided the original author(s) and source are credited.

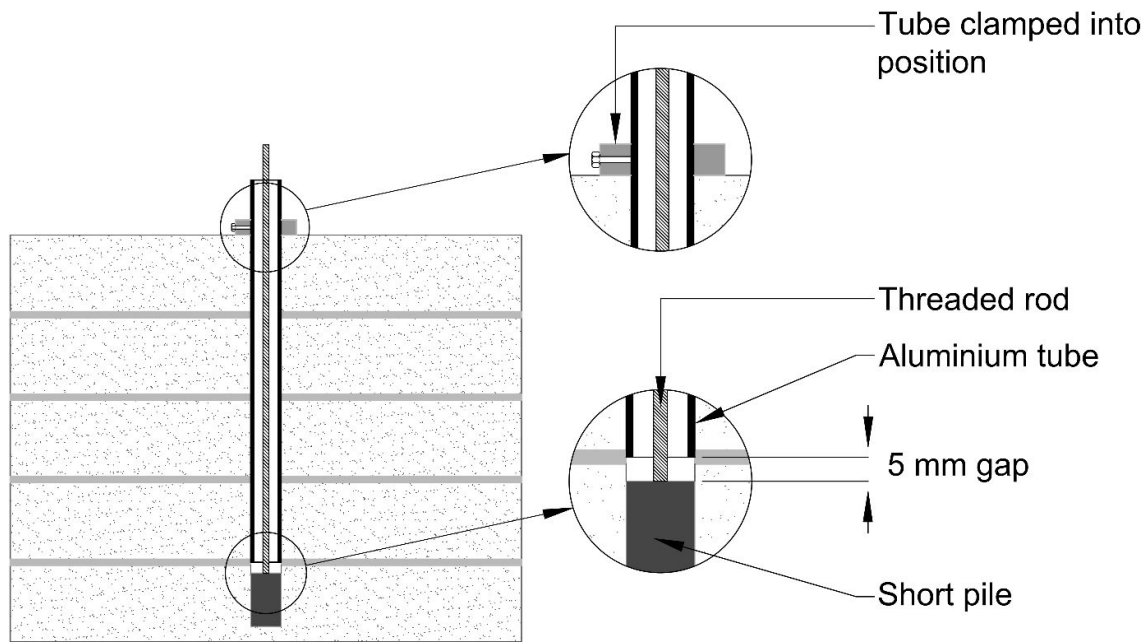


Fig. 4. Setup used to support augered holes behind piles

313

314

315

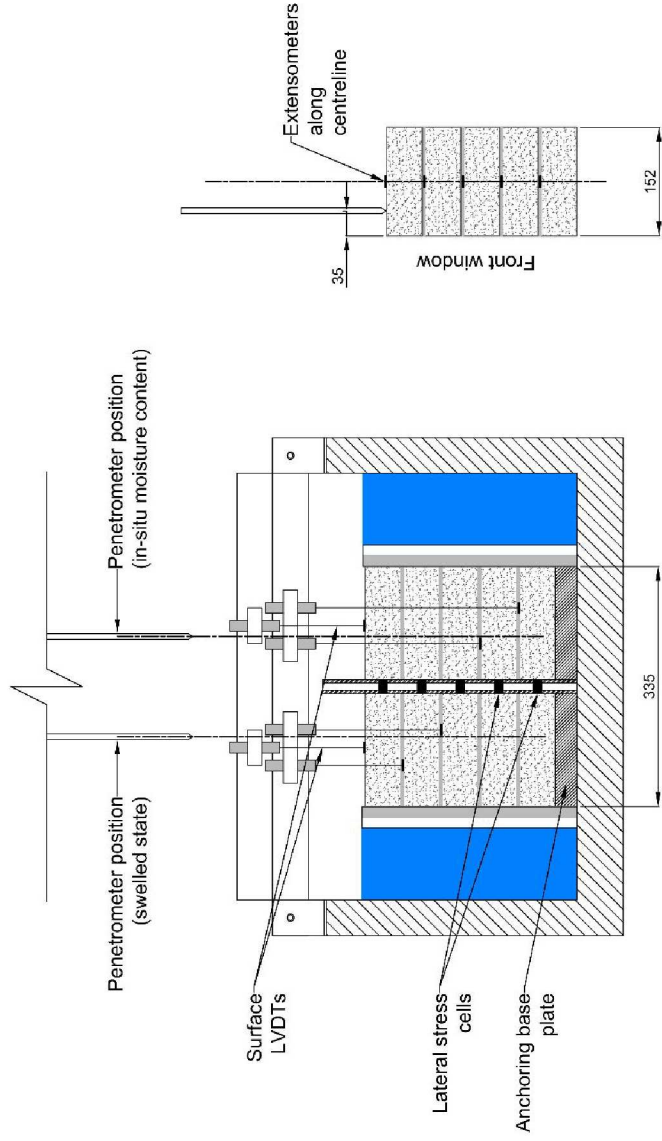
316 The layout of the final test is illustrated in Fig. 5. The test consisted of a single aluminium pile
 317 in the centre of the model (anchored at its base), instrumented with lateral load cells positioned
 318 at the centre of each clay layer. Measuring 19.05 mm in diameter, the pile was placed in a thin
 319 latex membrane (prior to being inserted into the pre-augured hole) to protect instrumentation
 320 from the water that would ultimately be introduced into the strongbox. The pile was then
 321 inserted (from the top of the profile) into an augered hole with a 20 mm diameter.

322

323 For the instrumented pile, the lateral load cells used were designed, based on an approach
 324 suggested by Jacobsz (2002). The load cells were manufactured from aluminium using a
 325 process referred to as electrical discharge machining (EDM). As shown in Fig. 6, the load cells
 326 comprised of two rounded surfaces and an inner web measuring 0.3 mm in thickness. This
 327 web was instrumented on either side with 1 k Ω strain gauges and wired into a full-Wheatstone
 328 bridge configuration. Once slotted into the aluminium pile, the rounded edges of the load cells
 329 fitted flush with the outer diameter of the pile as illustrated in Fig. 7.

330

OPEN ACCESS: This work (the Author's Accepted Manuscript) is licensed under a Creative Commons Attribution 4.0 International License (CC BY 4.0), which permits unrestricted use, distribution, and reproduction in in any medium, provided the original author(s) and source are credited.



331

332

333

Fig. 5. Instrumented pile test

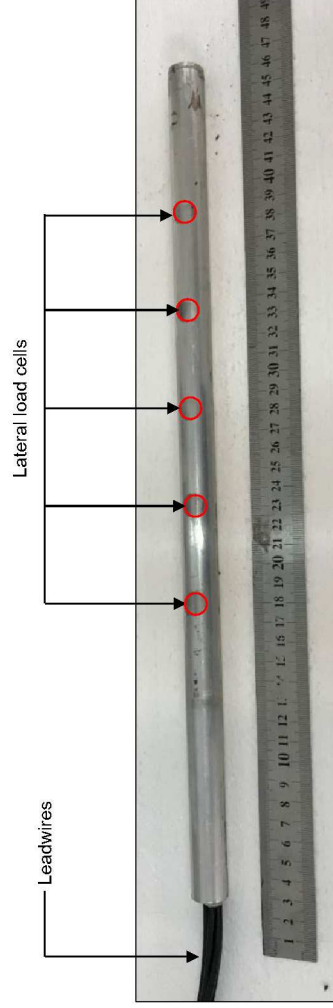


334

335

336

Fig. 6. Un-instrumented lateral load cells



337

338

339

Fig. 7. Assembled instrumented pile

340 This test sequence involved accelerating the model to the desired centrifugal acceleration of
341 30 *g* at the clay's in-situ water content. The strongbox was then flooded with water, inducing
342 swelling of the profile. Throughout the swell process, changes in lateral stresses against the
343 pile shaft were monitored. Additionally, strength measurements of the profile were performed
344 in-flight by means of cone penetration testing (CPT). CPTs were performed at the clay's in-
345 situ water content, and after the targeted swell magnitude had been achieved (that predicted
346 by Van der Merwe (1964) for a clay of *very high potential expansiveness*). The CPT
347 measurements for this test are presented in Fig. 8. Also included in Fig. 8, are CPT
348 measurements conducted in a greenfield centrifuge test (i.e. considering only a soil profile with
349 no external structures or loads) conducted on the same soil type for the same model layout
350 (Gaspar *et al.* 2023).

351

352 While holes were cut in the geotextiles to provide a path for the penetrometer to pass through,
353 the penetrometer punched through the bottom two geotextile layers during the instrumented
354 pile test, as indicated in Fig. 8. In Fig. 8 the prefixes "GF" and "IP" in the legend indicate the
355 greenfield and instrumented pile tests respectively.

356

357 From this figure, it can be seen that the penetration resistance reduced substantially during
358 the swell process. Furthermore, CPTs performed at the clay's in-situ water content and after
359 achieving the targeted swell are similar for the instrumented pile test and the greenfield test.

360 This finding provides confidence that the sample preparation procedure implemented for these
361 two tests, as well as for the pull-out tests discussed previously, produced specimens with
362 consistent strength. Similarly, it illustrates that any tests performed after achieving the targeted
363 swell were also carried out under comparable conditions. Key details of the four centrifuge
364 tests conducted are highlighted in Table 4.

365

366

OPEN ACCESS: This work (the Author’s Accepted Manuscript) is licensed under a Creative Commons Attribution 4.0 International License (CC BY 4.0), which permits unrestricted use, distribution, and reproduction in any medium, provided the original author(s) and source are credited.

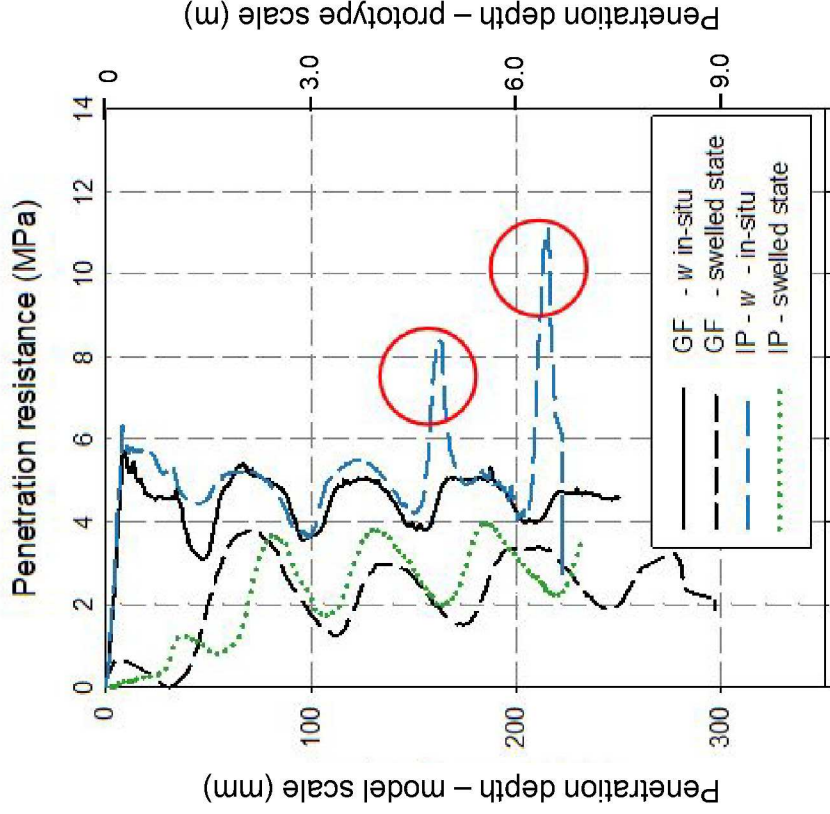


Fig. 8. Penetration results for the greenfield (GF) (after Gaspar *et al.* (2023)) and instrumented pile (IP) tests

367
 368
 369
 370
 371
 372
 373
 374
 375
 376
 377
 378
 379
 380
 381

382 **Table 4: Test program**

Test ID	Pile material	Pile dimensions	Pile dimensions	Testing period
		(model) – length (L); diameter (D) (mm)	(prototype) – length (L); diameter (D) (m)	
T1	Rapid	L = 35	L = 1.05	Before and after swell
	hardening grout	D = 20	D = 0.6	
T2	Rapid	L = 35	L = 1.05	After swell
	hardening grout	D = 20	D = 0.6	
T3_S	Rapid	L = 35	L = 1.05	After swell
	hardening grout with aluminium tube supporting holes	D = 20	D = 0.6	
T4_I	Aluminium	L = 355	L = 10.65	From in-situ water content, throughout swell process
	(instrumented)	D = 19	D = 0.57	

383

384 **Results**

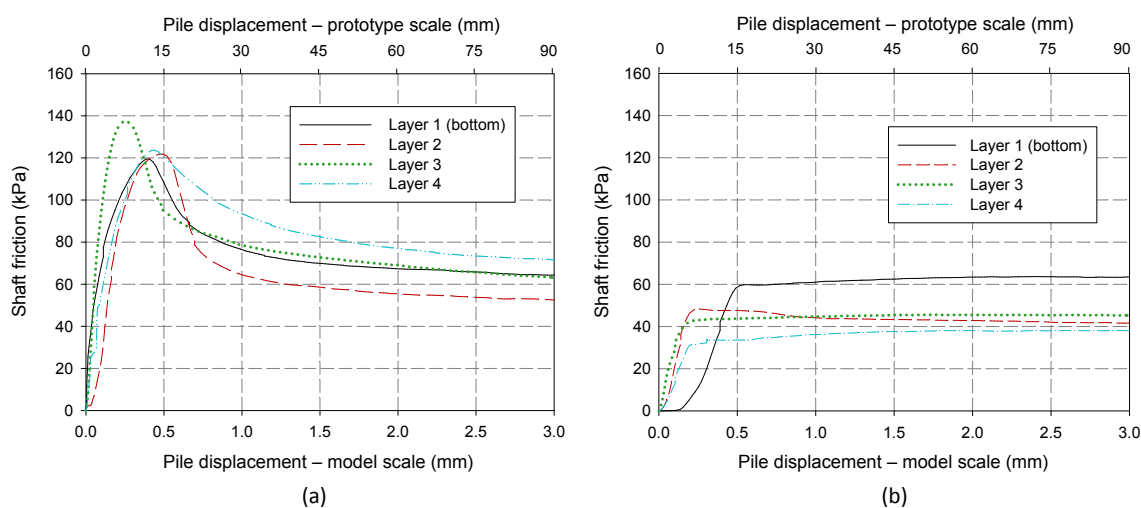
385 The results presented by Smit *et al.* (2019) revealed that the pull-out (shaft) capacity of full-
 386 length piles reduced after allowing swell to occur. The aim of the plug pull-out tests was to
 387 investigate the dependency of plug pull-out capacity on confinement (overburden) stress at
 388 various depths.

389

390 **Plug pull-out capacity (Test 1)**

391 This series of pull-out tests aimed to investigate the pull-out capacity of piles prior to swell, i.e.
 392 at the soil's in-situ water content. After obtaining the pull-out capacity of the plugs at their in-
 393 situ water content, the model was flooded to allow the targeted swell to be achieved. Once
 394 reached, the plugs were pulled a second time. Fig. 9 illustrates the mobilised shaft friction
 395 versus plug displacement during the pull-out tests, prior to and after swell.

396



397

398 **Fig. 9. Mobilised shaft friction versus pile displacement at a) the soils in-situ moisture content and b) after swell had**
 399 **occurred during pull-out tests**

400

401 From Fig. 9a) it can be seen that peak shaft friction was achieved at approximately 0.4 mm
 402 (0.02 pile diameter) displacement for all plugs except that in Layer 3, which reached its peak
 403 at approximately 0.25 mm (0.0125 pile diameter). Fig. 9a) illustrates that the peak shaft friction
 404 achieved appears independent of depth within the model and thus of confining pressure. Three
 405 of the piles consistently reached a peak shaft friction of approximately 120 kPa, with the plug
 406 in Layer 3 achieving a peak shaft friction of close to 140 kPa.

407

408 Fig. 9b) presents the pull-out results for the same plugs after the targeted swell had been
 409 reached. In this figure, no peak is observed, but rather all piles appear to reach a certain value
 410 of shaft friction and then remain constant. Since this figure presents the results of piles which
 411 were previously pulled out of the soil, it might be expected that the maximum shaft friction

412 attained with any further “pulling” would be equivalent to the residual value observed in Fig.
413 9a). This argument is supported by considering that a failure plane would already have been
414 established during the first pull-out test. However, upon closer inspection, it can be seen that
415 there are some differences between the maximum values of shaft friction attained in Fig. 9b)
416 and the values of residual friction observed in Fig. 9a). These differences can be attributed to
417 the softening that occurred during the swell process.

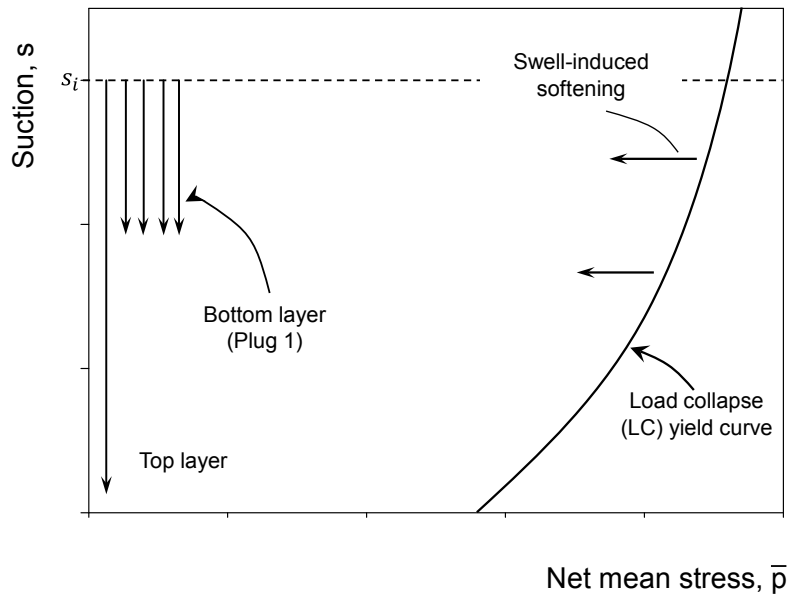
418

419 The largest difference is for the plug in the surface layer (Layer 4) where the lowest confining
420 stress of the 4 plugs would have been experienced. The smallest difference was for the plug
421 in Layer 1 at the bottom of the model (experiencing the highest confining stress). The result in
422 Fig. 9 can be interpreted within the extended Barcelona Basic Model for Expansive Clays
423 (BExM). For this interpretation, it is useful to consider Fig. 10 which highlights the stress state
424 at various positions in the profile in relation to the load collapse (LC) yield curve. In this figure,
425 all 4 layers begin at the same value of suction (s_i). The macroscopic expansion associated
426 with the reduction in suction results in soil softening, which can be represented as the
427 movement of the LC yield curve to the left. The extent of this movement is related to the
428 position of the initial stress state relative to the LC curve. For lower net-mean stresses, the
429 initial stress state is further from the LC curve and will therefore result in the most softening.

430

431 It should be noted that in Fig. 10, it has been assumed that the suction within the bottom 4
432 clay layers reduced by approximately the same amount. This is supported by the consistent
433 CPT measurements for these layers as presented in Fig. 8. As overburden stress increases
434 with depth, swell is incrementally restricted to a larger degree. For this reason, the magnitude
435 of swell-induced softening becomes negligible in the bottom layer, where very little swell
436 occurred. Conversely, in the top layer where the most swell was observed, the effects of swell-
437 induced softening produced the differences between the residual shaft friction in Fig. 9a) and
438 the peak shaft friction in Fig. 9b).

439



440

441

Fig. 10. Interpretation using the BExM framework

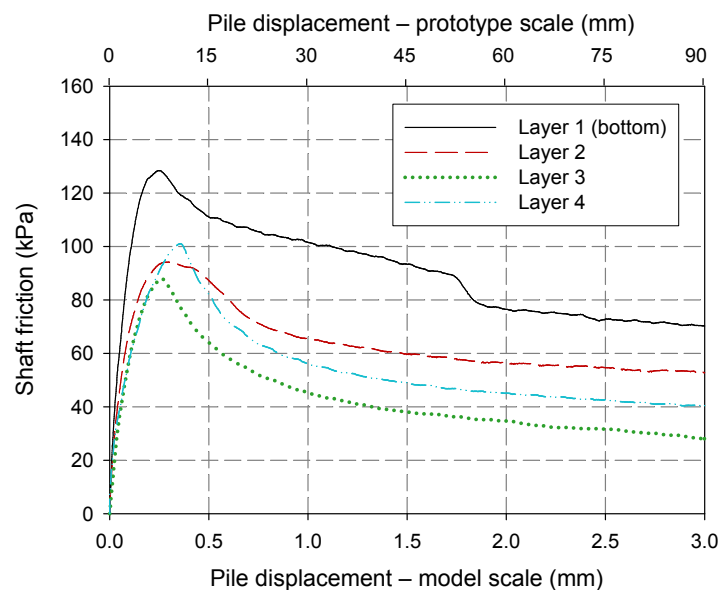
442

Plug pull-out (Test 2-after swell)

443 The model layout for Test 2 was identical to that presented in the previous section. However,
 444 for this test, plugs were only pulled once the targeted swell magnitude had been achieved, as
 445 opposed to pull-out at the in-situ moisture content in the previous test. Fig. 11 illustrates the
 446 results of this pull-out test.

447

448



449

450

Fig. 11. Pull-out test after swell (unsupported holes)

451

452 In the study conducted on full-length piles by Smit *et al.* (2019), it was found that the pull-out
453 (shaft) capacity reduced by approximately 60% following swelling. Similarly, the results
454 presented in Fig. 11 show a reduction in shaft resistance for all layers, except Layer 1 (at the
455 bottom of the model). In describing the possible mechanisms responsible for the observed
456 increase in pull-out capacity after swell, Blight (1984) attributed his finding to an increase in
457 lateral pressure against the piles. Conversely, Elsharief (2007) attributed the observed
458 reduction in shaft resistance after wetting, to post-swell softening.

459

460 The results of the centrifuge models presented thus far illustrate that there is a relationship
461 between overburden stress and the dominant mechanism governing pile shaft capacity after
462 swell. Closer to the surface, swell is allowed to occur more freely, and so swell-induced
463 softening is the dominant mechanism. At depth where swell is restricted by overburden stress,
464 so too is swell-induced softening and, as such, shaft capacity remains relatively unchanged
465 during and after the wetting process.

466

467 Fig. 12 illustrates a typical example of a plug just after being removed from the model. From
468 this photo, it is evident that during a pull-out test, failure occurs within the clay rather than
469 along the pile/soil interface as may be expected for a perfectly smooth (e.g. aluminium) pile.
470 This observation is in agreement with what was observed by Smit *et al.* (2019).

471

472

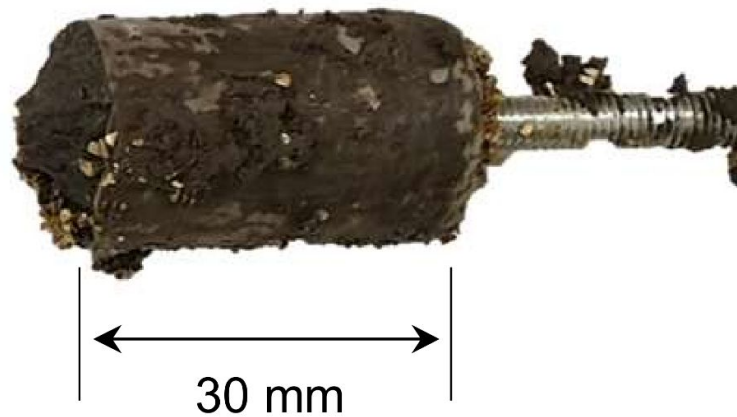


Fig. 12. Photograph of short length pile after being pulled out of a swelled profile

473

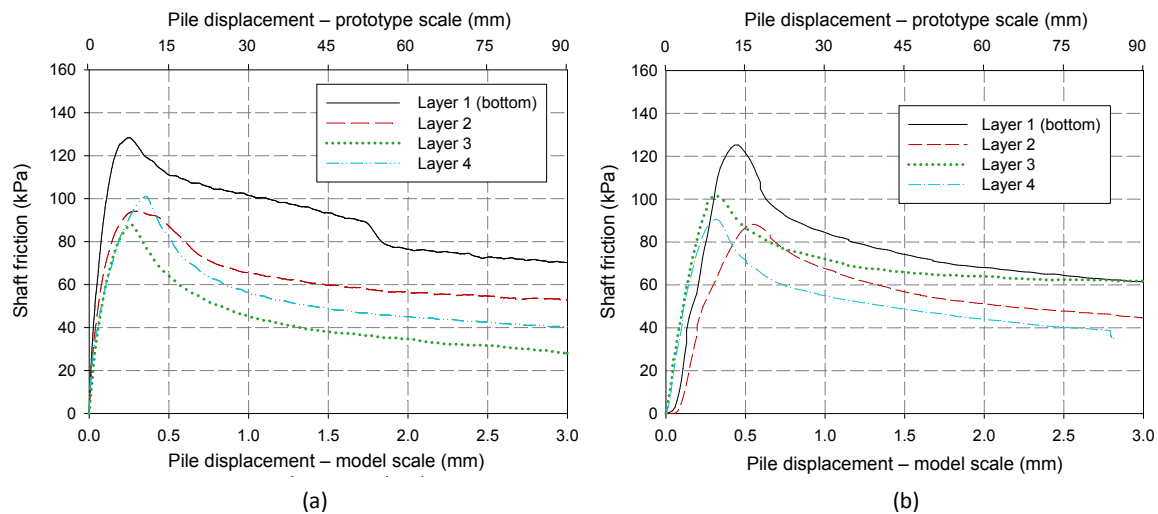
474

475

476 **Plug pull-out (Test 3 – after swell - supported holes)**

477 The final pull-out test had the same layout as the previous two tests, except for the fact that
 478 the holes above the plugs were supported with aluminium tubes. This test was performed to
 479 determine to what degree (if any) the clay which swelled above the plugs affected the
 480 measured pull-out (shaft) capacities. Fig. 13 presents the results of the two pull-out tests
 481 conducted after swell with and without supported holes.

482



483

484 Fig. 13. Plug pull-out tests conducted after achieving the targeted swell for a) unsupported holes and b) supported holes

485

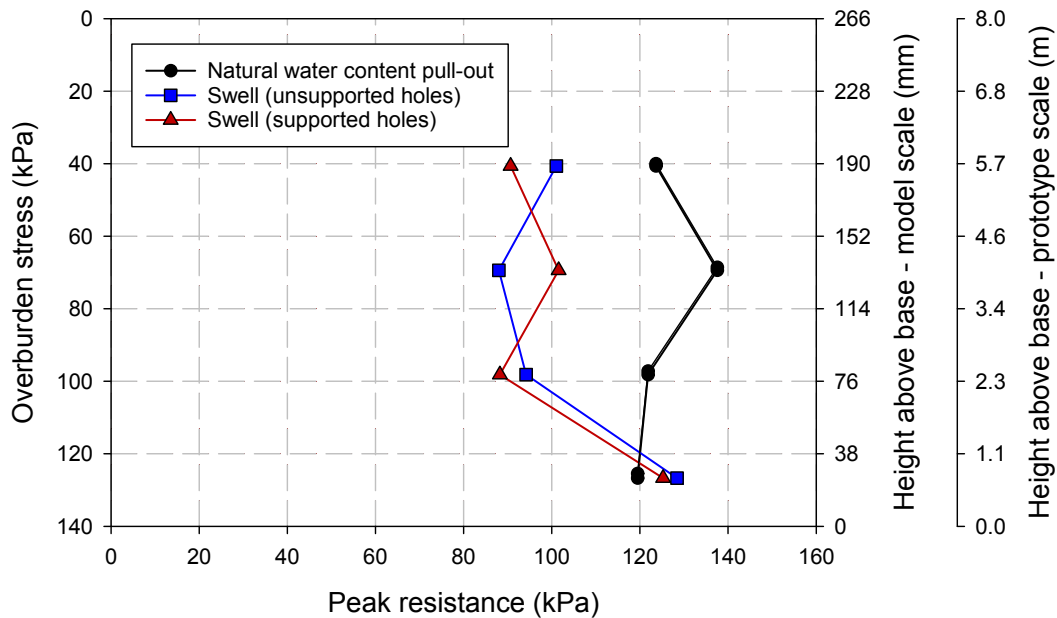
486 The result presented in Fig. 13 illustrates that the soil swelling above the plugs for the test with
 487 unsupported holes had a negligible effect on the measured peak shaft friction. This can be

488 attributed to the fact that the soil which was allowed to swell behind the plug had softened
 489 significantly.

490

491 Fig. 14 presents the results of peak shaft friction (i.e. pull-out capacity) for the various pull-out
 492 tests conducted. On the primary vertical axis (left) the overburden stress has been calculated
 493 from the initial unit weight of the various layers. The secondary vertical axis (right) illustrates
 494 the position of the plug as the height above the base of the model in model scale. A third
 495 vertical axis (far right) presents the height above the base of the model in prototype scale. The
 496 results of the pull-out tests have also been summarised in Table 5.

497



498

499

500

501

502

503

504

505

506

Fig. 14. Comparison of pull-out capacities for the various pull-out tests conducted

507 **Table 5: Summary of pull-out test results**

Test ID	Layer	Peak friction – before swell (kPa)	Residual friction – before swell (kPa)	Peak friction – after swell (kPa)	Residual friction – after swell (kPa)
T1	1	119.5	64.4	63.5	NA
	2	121.8	72.0	41.6	NA
	3	137.6	63.1	45.2	NA
	4	123.6	52.5	37.9	NA
T2	1	NA	NA	128.3	69.0
	2	NA	NA	94.3	52.7
	3	NA	NA	87.8	27.6
	4	NA	NA	101.0	39.9
T3_S	1	NA	NA	125.3	61.0
	2	NA	NA	88.2	44.3
	3	NA	NA	101.6	61.6
	4	NA	NA	90.7	38.8

508

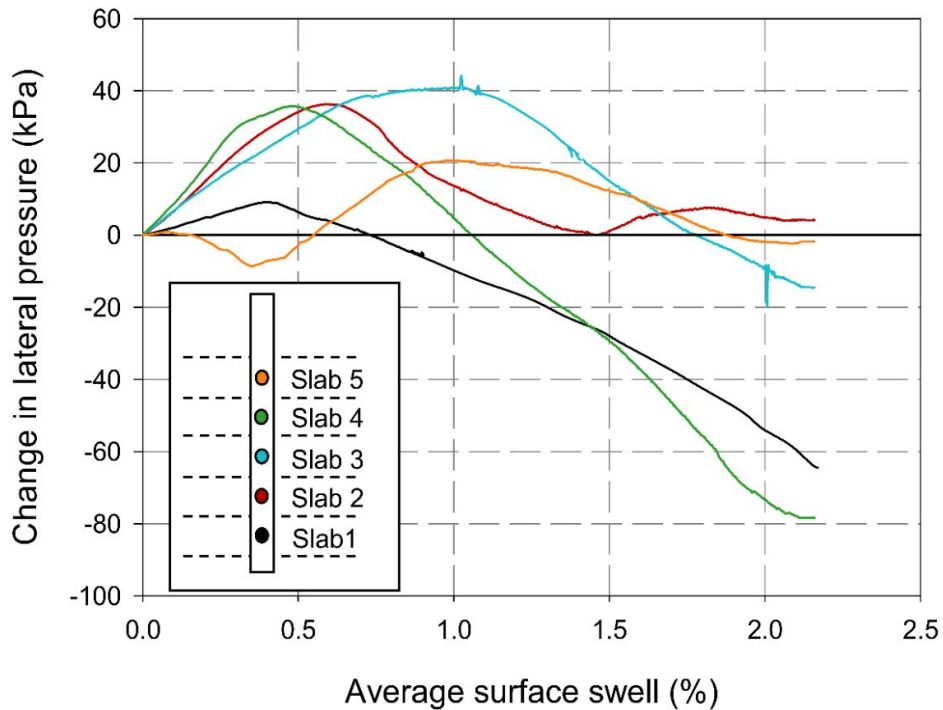
509 The results in Fig. 14 illustrate that in general, there is a reduction in pull-out capacity of piles
510 after allowing swell to occur. However, at high confining/overburden stresses, pull-out capacity
511 appears to be unchanged (and may increase locally) since the restriction of vertical swell
512 results in a reduction of swell-induced softening. Fig. 14 also illustrates good repeatability in
513 test results for piles pulled out after achieving targeted swell.

514

515 ***Instrumented pile test***

516 The purpose of this test was to measure changes in lateral swell pressure against the pile
517 shaft throughout the swell process. It should be highlighted that after installation, there was a
518 gap estimated at approximately 0.5 mm between the augered hole perimeter and the pile. As

519 a result, some expansion of the clay would have had to occur before contact was made with
 520 the pile. This is an important factor to recognise since any amount of heave can significantly
 521 reduce the magnitude of lateral swell-pressure against a structure (Fourie, 1991). For this
 522 reason, this test aimed to provide a qualitative illustration of the variation in swell pressure
 523 against the instrumented pile. The results of this test are provided in Fig. 15.
 524



525

526

527

Fig. 15. Change in lateral pressure due to swell

528 The results presented in Fig. 15 illustrate the *change* in lateral swell pressure against the pile.
 529 Data in this figure was zeroed after the model had been flooded. The data presented extends
 530 from the instant that the water level within the strongbox had cleared the top of the surface of
 531 the profile to the point at which the targeted swell had been achieved.

532

533 From Fig. 15 it can be seen that the top layer initially experienced a slight reduction in lateral
 534 pressure, followed by an increase to approximately 20 kPa. The initial drop in pressure or 'lag'
 535 before observing a pressure increase can be attributed to the fact that the aluminium pile was

536 pushed into the augered hole from the top of the profile. Doing so resulted in slight disturbance
537 of the adjacent soil, thereby creating a larger gap between the augered holes and the pile in
538 the top layer. However, the general trend observed for all load cells is that an increase in
539 lateral pressure occurs relatively early in the test, followed by a drop in pressure. This agrees
540 with the results of Schreiner and Burland (1991) of an oedometer test with lateral stress
541 measurement. It also supports the findings of Robertson and Wagener (1975) who observed
542 that the maximum swell induced lateral pressure against abutment walls occurred before
543 complete wetting was achieved.

544

545 The above finding also provides insights into the discrepancies in the publications of Blight
546 (1984) and Elsharief (2007) mentioned earlier. While Blight (1984) and Elsharief (2007)
547 reported an increase and reduction in shaft capacity respectively after wetting of the profile,
548 neither author stated the magnitude of swell that had occurred at the time of testing. A closer
549 investigation of these studies reveals wetting periods of 3-4 weeks (Blight 1984) and 2 months
550 (Elsharief 2007). Considering the results in Fig. 15, it is likely that the tests conducted by Blight
551 (1984) were conducted early in the swell process where there was still an increase in lateral
552 swell pressure against the pile. Similarly, the significantly longer wetting period of Elsharief
553 (2007) place the test in the later stages of the swelling process where swell induced softening
554 becomes the dominant mechanism.

555

556 It is therefore crucial that any tests which aim to investigate the shaft capacity of a pile after
557 swell has occurred, should be considered together with the anticipated magnitude of swell. By
558 not considering the magnitude of anticipated swell, it cannot be stated whether softening or
559 increases in lateral pressure will dominate the behaviour of the pile.

560

561 Even though the results presented in Fig. 15 are meant to provide qualitative illustrations of
562 the variation in lateral stress, the result does at first, appear contradictory to the results of the
563 plug pull-out tests presented previously. The end of the instrumented pile test represents the

564 level of swell at which plugs were pulled out of the profile for the previous tests. Whereas the
565 result presented in Fig. 14 illustrates a relatively unchanged value of pull-out capacity for the
566 bottom plug after swell when compared to the in-situ water content pull-out test, Fig. 15
567 illustrates a reduction in lateral stress in this clay layer. To reconcile these two results, it is
568 important to consider the absolute values of stress throughout the model. The initial
569 overburden stress at the bottom of the top layer and the bottom of the model is approximately
570 27 and 130 kPa respectively. As such, a unit reduction in lateral pressure at the latter stages
571 of a swell process will have a much more significant impact on the shaft capacity in upper
572 portions of the profile.

573

574 **Conclusions**

575 The results of the centrifuge tests presented in this study illustrate that the shaft (pull-out)
576 capacity of a pile after allowing swell to occur is dependent on both overburden stress (depth
577 in the profile) and on the magnitude of swell which has occurred. At the clay's in-situ water
578 content, pull-out tests revealed no dependency of shaft capacity on overburden stress.
579 However, after achieving a targeted value of swell (that predicted by Van der Merwe (1964)
580 for a clay of very high potential expansiveness), a reduction in pull-out capacity was observed
581 in the upper portions of the clay profile. This reduction in capacity can be attributed to swell-
582 induced softening of the surrounding clay. Conversely, for short-length piles (plugs) tested at
583 higher confining stresses, pull-out capacity remained relatively unchanged when compared to
584 that measured under in-situ moisture conditions. An explanation for this finding is that at depth,
585 where swell is largely restricted, so too are the effects of swell-induced softening.

586

587 In addition to the dependency on overburden stress, it was found that the change in lateral
588 stresses against a pile is strongly dependent on the magnitude of heave which has occurred.
589 Regardless of the position within a profile, lateral stresses tend to increase in the early stages
590 of a swelling process and then reduce as heave continues. The lowest value of shaft
591 resistance throughout the lifetime of a structure may either be at the clay's in-situ moisture

592 content, or after a significant magnitude of heave has occurred. If site tests are conducted to
593 determine the shaft resistance of piles in expansive clays, an estimate of the likely magnitude
594 of heave and its variation with depth during the lifetime of the structure is required to achieve
595 a conservative design.

596

597 **Acknowledgements**

598 This work was funded by the UK Engineering and Physical Sciences Research Council
599 (EPSRC) under the Global Challenges Fund programme for a project entitled 'Developing
600 Performance based design for foundations of wind turbines in Africa (WindAfrica)', Grant Ref:
601 EP/P029434/1. The first author would also like to acknowledge the Newton Fund
602 UnsatPractice PhD exchange programme (grant Ref: ES/N013905/1), which enabled him to
603 spend six months at Durham University during his PhD study at the University of Pretoria. The
604 author's would also like to thank Corinus Claasen and Johan van Staden from Loadtech
605 Loadcells (Centurion) who assisted with the manufacturing of the instrumented pile presented
606 in this study.

607

608 **Competing interests:** The authors declare there are no competing interests.

609 **Authors contribution statement:**

610 Tiago Gaspar: Conceptualization; Methodology; Formal analysis; Investigation; Writing –
611 Original Draft; Visualization

612 Schalk Jacobsz: Conceptualization; Supervision; Funding acquisition; Writing – Review and
613 Editing; Project administration

614 Gerrit Smit: Conceptualization; Methodology; Writing – Review and Editing

615 Ashraf Osman: Conceptualization; Funding acquisition; Writing – Review and Editing; Project
616 administration

617

618 **Funding contribution statement:** This research was supported by the UK Engineering and
619 Physical Sciences Research Council (EPSRC) under the Global Challenges Fund programme

620 for a project entitled 'Developing Performance based design for foundations of wind turbines
621 in Africa (WindAfrica)', Grant Ref: EP/P029434/1. The first author would also like to
622 acknowledge the Newton Fund UnsatPractice PhD exchange programme (grant Ref:
623 ES/N013905/1), which enabled him to spend six months at Durham University during his PhD
624 study at the University of Pretoria.

625 **Data availability statement:** Data generated or analysed during this study are available from
626 the corresponding author upon reasonable request.

627

628 *References*

629 ASTM (2014a). ASTM D854–14: Standard Test Methods for Specific Gravity of Soil Solids by
630 Water Pycnometer, West Conshohocken, P.A.

631

632 ASTM (2014b). ASTM D4546–14: Standard Test Method for One-Dimensional Swell or
633 Collapse of Soils, Technical report, West Conshohocken, P. A.

634

635 ASTM (2017a). ASTM D6913 / D6913M-17: Standard Test Methods for Particle-Size
636 Distribution (Gradation) of Soils Using Sieve Analysis, West Conshohocken, P.A.

637

638 ASTM (2017b). ASTM D7928-17: Standard Test Method for Particle-Size Distribution
639 (Gradation) of Fine-Grained Soils Using the Sedimentation (Hydrometer) Analysis, West
640 Conshohocken, PA.

641

642 ASTM (2017c). ASTM D4318-17e1: Standard Test Methods for Liquid Limit, Plastic Limit, and
643 Plasticity Index of Soils, West Conshohocken, P. A.

644

645 ASTM (2017d). ASTM D2487-17e1: Standard Practice for Classification of Soils for
646 Engineering Purposes (Unified Soil Classification System), West Conshohocken, P. A.

647

- 648 Blight, G. E. (1984). Power Station Foundations in Deep Expansive Soil Power Station
649 Foundations in Deep Expansive Soil. *First International Conference on Case Histories in*
650 *Geotechnical Engineering*, Missouri, pp. 77–86.
- 651
- 652 Brackley, I. J. A. B. (1975b). A model of unsaturated clay structure and its application to swell
653 behaviour. *Proceedings of the 6th African Regional Conference on Soil Mechanics and*
654 *Foundation Engineering*, Vol. 1, pp. 65–70.
- 655
- 656 Byrne, G., Chang, N. and Raju, V. (2019). A Guide to Practical Geotechnical Engineering in
657 Africa, 5th Edition edn, FRANKI A KELLER COMPANY.
- 658
- 659 Charlie, W. A., Osman, M. A. and Elfatih, M. A. (1985). Construction on expansive soils in
660 Sudan. *Journal of Construction Engineering and Management*, 110 No. 3, 359-374
- 661
- 662 Day, P. (2017). Challenges and shortcomings in geotechnical engineering practice in the
663 context of a developing country (Terzaghi Oration). *Proceedings of the 19th International*
664 *Conference on Soil Mechanics and Geotechnical Engineering*, Seoul, pp. 11-34.
- 665
- 666 Elsharief, A. M., Ahmed, E. O. and Mohamedzein, Y. E. A. (2007). Guidelines for the Design
667 of Bored Concrete Piles in Expansive Soils of Sudan. *Graduate School Conference, on Basic*
668 *Sciences and Engineering*, University of Khartoum.
- 669
- 670 Elsharief, A. (2012). Foundations on Expansive Soils, Sudan Experience. *Graduate School*
671 *Conference, on Basic Sciences and Engineering*, University of Khartoum.
- 672
- 673 Fleming, K., Weltman, A., Randolph, M. and Elson, K. (2009). Piling Engineering, 3rd edn,
674 Taylor & Francis.
- 675

676 Fourie, A. B. (1991). Lateral swelling pressure developed in an active clay. *Geotechnics in the*
677 *African Environment*, Maseru, Lesotho, (eds G. E. Blight, A. B. Fourie, I. Luker, D. J. Mouton
678 and R. J. Scheurenberg), Vol. 1, pp. 267–274 Balkema, Rotterdam, Maseru, Lesotho.

679

680 Fredlund, D. G. (1983). Prediction of ground movements in swelling clays. *31st Annual Soil*
681 *Mechanics and Found Engineering Conference*. University of Minnesota, Minneapolis.

682

683 Gaspar, T. A. V., Jacobsz, S. W., Heymann, G., Toll, D. G., Gens, A., and Osman, A. S.
684 (2022). The mechanical properties of a high plasticity expansive clay. *Engineering Geology*,
685 303(March), 106647. <https://doi.org/10.1016/j.enggeo.2022.106647>

686

687 Gaspar, T. A. V., Jacobsz, S. W., Smit, G., Gens, A., Toll, D. G., and Osman, A. S. (2023).
688 Centrifuge modelling of an expansive clay profile using artificial fissuring to accelerate swell.
689 *Engineering Geology*, 312, 106928. <https://doi.org/10.1016/j.enggeo.2022.106928>

690

691 Gaspar, T.A.V. (2020). *Centrifuge modelling of piled foundations in swelling clays*. PhD
692 Thesis, University of Pretoria, Pretoria, South Africa

693

694 Gens, A. and Alonso, E. E. (1992). A framework for the behaviour of unsaturated expansive
695 clays. *Canadian Geotechnical Journal* **29**, No. 6, 1013–1032.

696

697 Jacobsz, S. W. (2002). The effects of tunnelling on piled foundations, PhD thesis, University
698 of Cambridge September.

699

700 Jennings, J. E. and Kerrich, J. E. (1962). The heaving of buildings and the associated
701 economic consequences with particular reference to the Orange Free State Goldfields. *The*
702 *Civil Engineer in South Africa* **4** No. 11, 221–248.

- 703
- 704 Li, J., Cameron, D. and Ren, G. (2014). Case study and back analysis of a residential building
705 damaged by expansive soils. *Computers and Geotechnics*, **56**, 89–99.
- 706
- 707 Louw, H., Kearsley, E., and Jacobsz, S. W. (2020). Modelling horizontally loaded reinforced-
708 concrete piles in a geotechnical centrifuge. *International Journal of Physical Modelling in*
709 *Geotechnics* **22** No.1, 14-25
- 710
- 711 Manca, D., Ferrari, A., and Laloui, L. (2016). Fabric evolution and the related swelling
712 behaviour of a sand/bentonite mixture upon hydro-chemo-mechanical loadings.
713 *Géotechnique*, *66*(1), pp. 41–57. <https://doi.org/10.1680/jgeot.15.P.073>
- 714
- 715 Monroy, R., Zdravkovic, L., and Ridley, A. M. (2015). Mechanical behaviour of unsaturated
716 expansive clay under K0 conditions. *Engineering Geology*, *197*, pp. 112–131.
717 <https://doi.org/10.1016/j.enggeo.2015.08.006>
- 718
- 719 Moses, A. M. (2008). Mineralogy, Chemistry and Pedological Investigations of the
720 Maandaagshoek 254 kt's Palygorskite deposit: Implication on the Genesis and Industrial
721 Application (Honours report). *University of Pretoria*, Pretoria.
- 722
- 723 Meintjes, H. A. C. (1991). A case history on heaving clay: Colinda Primary School.
724 *Geotechnics in the African Environment*, Maseru, Lesotho, (eds G. E. Blight, A. B. Fourie, I.
725 Luker, D. J. Mouton and R. J. Scheurenberg) pp. 99–104. Balkema, Rotterdam.
- 726
- 727 Nelson, J. D., Reichler, D. K. and Cumbers, J. M. (2006). Parameters for heave prediction by
728 oedometer tests. *Proceedings of the 4th International Conference on Unsaturated Soils*,
729 Carefree, Arizona, pp. 951–961.

730

731 Pellissier, J. P. (1997). A raft design method for swelling clay. *Proceedings of the 14th*
732 *International Conference on Soil Mechanics and Foundations Engineering*. Hamberg,
733 Germany, pp. 863–869.

734

735 Robertson, A. and Wagener, F. (1975). Lateral swelling pressures in active clay. *Proceedings*
736 *of the 6th African Regional Conference on Soil Mechanics and Foundation Engineering*, vol.
737 1, Durban, pp. 107–114.

738

739 Schreiner, H. D. (1988). *Volume Change of Compacted Highly Plastic African Clays*, PhD
740 thesis, Imperial College London.

741

742 Schreiner, H. D. and Burland, J. B. (1991). A comparison of three swell test procedures.
743 *Geotechnics in the African Environment*, Maseru, Lesotho, (eds G. E. Blight, A. B. Fourie, I.
744 Luker, D. J. Mouton and R. J. Scheurenberg), pp. 259–266, Balkema, Rotterdam

745

746 Smit, G., Gaspar, T. A. V., Jacobsz, S. W. and Osman, A. S. (2019). Centrifuge modelling of
747 pile pull-out tests in expansive soil. *XVII European Conference on Soil Mechanics and*
748 *Geotechnical Engineering*, Reykjavik, Iceland.

749

750 Van der Merwe, D. (1964). The prediction of heave from the plasticity index and percentage
751 clay fraction of soils. *The Civil Engineer* pp. 103–107.

752